REPORT DOCUMENTATION PAGE

Form Approved
OMB No. 0704-0188

1. REPORT DATE *(DD-MM-YYYY)*	**2. REPORT TYPE**	**3. DATES COVERED** *(From - To)*
21-08-2007	Technical Paper	

4. TITLE AND SUBTITLE

Preliminary Results on Coaxial Jets Spread Angles and the Effects of Variable Phase Transverse Acoustic Fields

5a. CONTRACT NUMBER

5b. GRANT NUMBER

5c. PROGRAM ELEMENT NUMBER

6. AUTHOR(S)
Ivett A. Leyva & Douglas Talley (AFRL/RZSA); Juan I. Rodriguez (UCLA); Bruce Chehroudi (ERC)

5d. PROJECT NUMBER

5e. TASK NUMBER
23080533

5f. WORK UNIT NUMBER

7. PERFORMING ORGANIZATION NAME(S) AND ADDRESS(ES)

Air Force Research Laboratory (AFMC)
AFRL/RZSA
10 E. Saturn Blvd.
Edwards AFB CA 93524-7680

8. PERFORMING ORGANIZATION REPORT NUMBER

AFRL-RZ-ED-TP-2007-528

9. SPONSORING / MONITORING AGENCY NAME(S) AND ADDRESS(ES)

Air Force Research Laboratory (AFMC)
AFRL/RZS
5 Pollux Drive
Edwards AFB CA 93524-7048

10. SPONSOR/MONITOR'S ACRONYM(S)

11. SPONSOR/MONITOR'S NUMBER(S)
AFRL-RZ-ED-TP-2007-528

12. DISTRIBUTION / AVAILABILITY STATEMENT

Approved for public release; distribution unlimited (PA #07462A).

13. SUPPLEMENTARY NOTES

Presented at the 46th AIAA Aerospace Sciences Meeting and Exhibit (ASME), Reno, NV, 7-10 January 2008 (AIAA 2008-950).

14. ABSTRACT

An experimental study on the jet spreading angle of N2 shear coaxial jets at sub-, near-, and supercritical pressures is presented. The jet spreading angle is an important parameter which characterizes the mixing between two flows forming a shear layer. The present results are compared with previous experimental data, CFD results, and theoretical predictions. The angle measurements are made directly from at least 20 backlit images. The shear coaxial injector used here is similar to those used in cryogenic liquid rockets. The chamber pressure ranges from 1.5 to 5.0 MPa to span subcritical to supercritical pressures. The chamber to outer jet density ratio varies from 0.17-4.8 and the momentum flux ratio between the outer and the inner jet varies from 0.37 to 30. These ratios are mainly varied by changing the temperature and flow rates of the outer jet. For the ranges of conditions studied it is found that the tangent of the jet spreading angle is roughly constant and approximately 0.19 with std. dev. of 0.02. The value is lower than those predicted by different theories for planar mixing layers of variable density for gaseous flows. The second part of the paper focuses on the initial results obtained by combining two piezo-sirens which generate a transverse acoustic field to excite the coaxial jet. The resonant frequency studied is ~3kHz and $\Delta P/P$ varies from 1-1.6%. These two acoustic sources can have an arbitrary phase between them so the position of the jet with respect to the pressure and velocity field can be adjusted. The main parameter investigated is the length of the dark inner jet core. The initial results indicate an effect of the phase angle on the dark core length but the differences are statistically significant only in the extreme cases.

15. SUBJECT TERMS

16. SECURITY CLASSIFICATION OF:			**17. LIMITATION OF ABSTRACT**	**18. NUMBER OF PAGES**	**19a. NAME OF RESPONSIBLE PERSON**
					Douglas Talley
a. REPORT	**b. ABSTRACT**	**c. THIS PAGE**	SAR	16	**19b. TELEPHONE NUMBER** *(include area code)*
Unclassified	**Unclassified**	**Unclassified**			N/A

46th AIAA Aerospace Sciences Meeting and Exhibit
7 - 10 January 2008, Reno, Nevada

AIAA 2008-950

Preliminary Results on Coaxial Jet Spread Angles and the Effects of Variable Phase Transverse Acoustic Fields

Ivett A. Leyva[1], Juan I Rodriguez[2], Bruce Chehroudi[3] and Douglas Talley[4]
Air Force Research Laboratory, Edwards AFB, CA 93524

An experimental study on the jet spreading angle of N_2 shear coaxial jets at sub-, trans-, and supercritical pressures is presented. The jet spreading angle is an important parameter which characterizes the mixing between two flows forming a shear layer. The present results are compared with previous experimental data, CFD results, and theoretical predictions. The angle measurements are made directly from at least 20 backlit images. The shear coaxial injector used here is similar to those used in cryogenic liquid rockets. The chamber pressure ranges from 1.5 to 5.0 MPa to span subcritical to supercritical pressures. The chamber to outer jet density ratio varies from 0.20 to 0.93 and the momentum flux ratio between the outer and the inner jet varies from 0.36 to 30. These ratios are mainly varied by changing the temperature and flow rates of the outer jet. For the range of conditions studied it is found that the tangent of the jet spreading angle is roughly constant and approximately 0.19 with standard deviation of 0.02. The value is lower than those predicted by different theories for 2D mixing layers of variable density for gaseous flows. The second part of the paper focuses on the initial results obtained by combining two piezo-sirens which generate a transverse acoustic field to excite the coaxial jet. The resonant frequency studied is ~3kHz and ΔP/P varies from 0.7 to 1.3%. These two acoustic sources can have an arbitrary phase between them so the position of the jet with respect to the pressure and velocity fields can be adjusted. The main parameter investigated is the length of the dark inner jet core. The initial results indicate an effect of the phase angle on the dark core length but the differences are statistically significant only in the extreme cases.

Nomenclature

D	=	diameter with subscripts
L	=	axial dark core length
Lt	=	total or curved dark core length
MR	=	outer to inner jet momentum flux ratio
VR	=	outer to inner jet velocity ratio
T	=	temperature
P	=	pressure
Subscripts		
ch	=	chamber
v	=	visual (jet spreading angle)
w	=	vorticity (jet spreading angle)
OJ	=	outer jet
IJ	=	inner jet

[1] Lead, Combustion Group, AFRL/RZSA, Edwards AFB, CA 93524, AIAA Senior Member.
[2] Graduate Student, UCLA/ AFRL, Edwards AFB, CA 93524, AIAA Student Member.
[3] Principal Scientist, ERC Inc., AFRL, Edwards AFB, CA 93524, AIAA Member.
[4] Sr. Aerospace Engineer, AFRL/RZSA, Edwards AFB, CA 93524, AIAA Member.

I. Introduction

COAXIAL jet flows are of great interest to the rocket community because they are widely used in liquid rocket engines LRE's (e.g. Space Shuttle Main Engine (SSME)). A key advantage of coaxial jets is that as the Momentum Flux Ratio (MR) between the outer jet and the inner jet increases mixing between the two jets increases and mixing to certain uniformity can be obtained in relatively short distances from the exit plane. As LRE's have evolved into higher specific impulse designs with chamber pressures reaching supercritical values for some propellants, it is important to characterize coaxial flows at conditions spanning sub to supercritical pressures. The SSME and the Vulcan engine for the Ariane 5 launch vehicles are examples of LRE's designed to operate above the critical pressures of each propellant individually. In a typical application of a coaxial injector for a LOX/LH2 engine, the oxygen is injected at subcritical temperatures in the center jet while the hydrogen is injected at supercritical temperatures, after being used as a coolant for the engine nozzle, in the coaxial jet. A typical velocity ratio between the outer and inner jets is about 10[1]. For these flows, the mixture no longer has a singular critical point but rather there are critical mixing lines that define its thermodynamic state[1]. Because of the added complexity introduced when working with mixtures, N_2 is used as the sole working fluid in this study.

The growth of shear layers between two planar flows has been studied for decades since the rate of growth of the shear layer is indicative of the mixing process between the two layers. Of relevance here is the work of Brown and Roshko[2], who proposed an equation for the growth rate of the shear layer for subsonic two-dimensional incompressible turbulent gas-gas flows. Papamoschou and Roshko[3] also proposed an equation for the growth of the visual thickness of the shear layer for sub- to supersonic two-dimensional turbulent mixing layers. Dimotakis[4] proposed an equation for the vorticity growth rate of a planar freejet. Chehroudi et. al.[5] performed a comprehensive experimental study of single round jets at sub to supercritical pressures. They also compiled experimental data from different researchers presenting a data set that spans four orders of magnitude in the ratio of the chamber density to the jet density, which is the relevant parameter for single jets ejecting into a quiescent environment. He showed for the first time that for jets at supercritical pressure and temperature, the spreading angle agrees quantitatively with that predicted by the works mentioned above which were derived for incompressible variable-density gas-gas jets. The data from the present study will be compared to the above mentioned body of work.

The second part of the paper is focused on the effects of both the magnitude and phase of the acoustic pressure and velocity field on the coaxial jet flow. So far in the previous experiments performed in this lab there was one acoustic resonator at one end of the test chamber and a non-movable reflective wall at the other end. This meant that the relation of the position of the jet with respect to the acoustic wave profile was fixed. The amplitude of the pressure oscillations could be varied but to achieve the highest ratios of acoustic pressure vs. mean chamber pressure the custom was to run at the highest magnitude possible. By adding a second identical resonator the magnitude and relative position of the jet with respect to the pressure and velocity acoustic field can now be varied. We chose to start this study at subcritical pressures with MR~ 1 and 3 since we found in previous studies by Leyva et. al.[6,7] that the effects of acoustics on the dark core length were greatest at subcritical pressures and for $1<MR<4$. The length of the dark core, both the axial length and the total or curved length are the first metric we studied for this problem.

II. Experimental Setup

These experiments were carried out at the Cryogenic Supercritical Laboratory (EC-4) at the Air Force Research Laboratory (AFRL) at Edwards Air Force Base, CA. An overview of the facility is shown in Fig. 1. The setup with only one acoustic source is shown in Fig. 1A and the new setup with two acoustic sources is shown in Figure 1B. For either configuration, gaseous N_2 is used to supply the inner and outer jet flows and to pressurize the chamber. The outer and inner jets are cooled by two or three heat exchangers (HE's) depending on the plumbing configuration run. The coolant for both the inner and outer jet is liquid nitrogen obtained from a cryogenic tank. One heat exchanger cools the inner jet and the other two cool the outer jet. The temperature (T) of the two jets is controlled by adjusting the flow rate of liquid nitrogen through the HE's. The mass flow rate through the inner and outer jets is measured, before they are cooled, with Porter mass flow meters (122 and 123-DKASVDAA). It was found that it is much easier to measure the flow rates at ambient rather than at cryogenic temperatures. The chamber pressure is

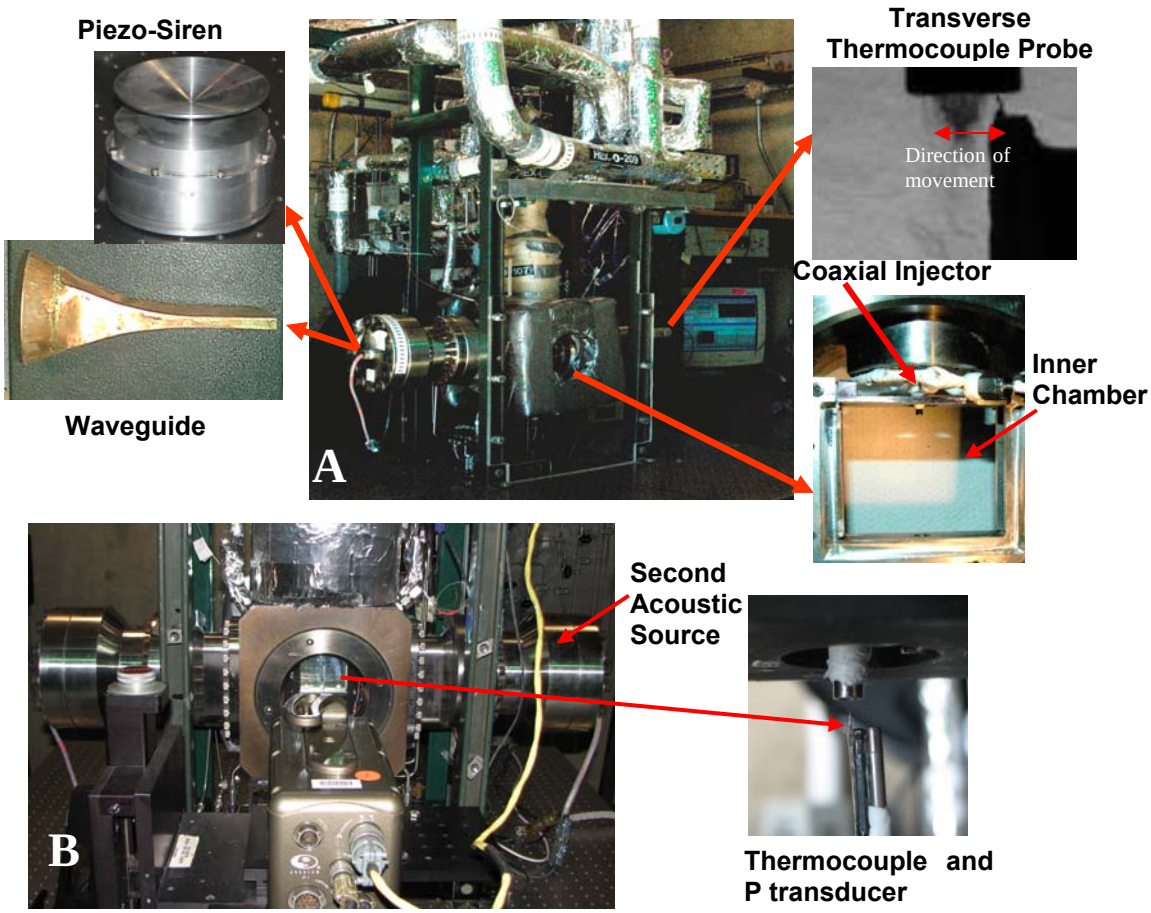

Figure 1. Overview of the Supercritical Flow Facility, EC-4 at AFRL/Edwards used for this study. A. Configuration with one acoustic source. B. Two acoustic sources.

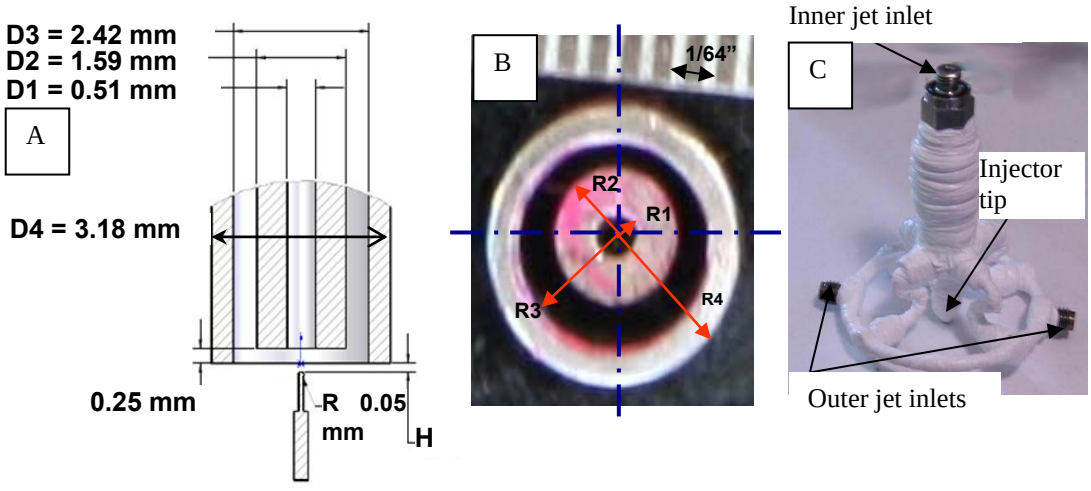

Figure 2. Details on the coaxial injector used for the present study

measured with a Stellar 1500 transducer. To keep the amplitude of the acoustic oscillations to a maximum near the jet, an inner chamber was created (Fig. 1). The inner chamber has nominal height of 6.6cm, width 7.6cm and depth 1.3cm. Details for the coaxial injector used are shown in Fig. 2. The inner diameter of the inner jet, D1, is 0.51 mm. The outer jet has an inner diameter, D2, of 1.59 mm and outer diameter, D3, of 2.42 mm. The length to inside diameter ratio is 100 for the inner jet and 67 for the outer jet (taking as reference the mean width of the annular passage). There is a small bias of about 8% of the mean gap width. The inner jet is recessed by 0.3 mm from the outer jet.

The temperature of the jets is measured with an unshielded type E thermocouple which has a bead diameter of 0.1mm. The accuracy of this thermocouple was checked with an RTD and found to be ±1K. With only one acoustic generator present the thermocouple is traversed across the outer and inner jets to obtain a reading as close as possible to the injector exit plane (also seen in Fig. 1A). The average distance from the exit plane, denoted H in Fig. 2 is ~0.3mm. However for the case where two acoustic sources are present the thermocouple is introduced from the bottom of the chamber so it can get as close to the exit plane as possible. In fact, the thermocouple can measure the temperature within the recess of the inner jet. As can be seen from Fig. 1B a Kulite XQC-062 pressure transducer is used to measure the pressure at a sampling frequency of 20kHz. Both the pressure transducer and the thermocouple are moved in the plane perpendicular to the jet axis with a piezo positioning system built by Atto cube which can move a total distance of about 3mm in 1 dimension. Properties such as density, viscosity, and surface tension are computed from the measured flow rates, chamber pressure and jet temperature, using NIST's REFPROP[8]. From this, the Re, We, VR and MR for a given condition can be computed.

The jet is visualized by taking backlit images using a Phantom 7.1 CMOS camera. The images have 128x256 pixels or 128x200 pixels, and each pixel represents an area of about 0.08mmx0.08mm. The framing rate was either 20kHz or 41kHz. The exposure time varies from 1-9μs. The jet is backlit using a Newport variable power arc lamp set at 160 or 300W. The acoustic waves are generated using one or two piezo-sirens custom-designed for AFRL by Hersh Acoustical Engineering, Inc. (Fig.1). For these acoustic sources a piezo-ceramic element is externally excited with a sinusoidal wave at the desired driving frequency for the system. This frequency is chosen by manually varying the frequency on a signal generator until the highest amplitudes for the pressure waves are obtained. This signal is amplified and then fed to the piezo-siren. The movement of the piezo element is transmitted to the aluminum cone attached to it, and the cone then produces acoustics waves. To accommodate for the rectangular chamber a waveguide with a catenary contour is used to guide the waves from a circular cross-section to a rectangular cross-section (also shown in Fig.1). The RMS of the acoustic pressure oscillations in the inner chamber ranges from ~1.5 to 3 psi at ~3.0 kHz.

III. Results and Discussion

A. Outer Jet Spreading Angle

The data for the spreading angle consists of 19 experimental data points spanning chamber pressures from 1.5 to 5.0 MPa. For reference the critical P and T for N_2 are 3.40 MPa, and 126.26 K respectively. The details of the test conditions are presented in the Appendix. A summary of the range of conditions tested is shown in Table 1. From these conditions one can see that at the subcritical pressures, the inner jet temperature is either a few degrees below or at the saturation temperature and the outer jet is a gas, therefore we have a two-phase coaxial flow exiting into a quiescent gas. For the other two pressures, both the inner and the outer jet are in the supercritical region and therefore these are one-phase coaxial flows issuing into a stagnant supercritical fluid. Even though both gas-gas and supercritical-supercritical flows are one-phase flows we want to distinguish between them since in this work we do not have gas-gas coaxial jets, which is what most people have reported in the literature for coaxial jets. The jet spread angle between the outer jet and the chamber was measured directly from the backlit images. At least 20 images were measured manually by two people. It was found that for most cases the jet does not start growing from the exit plane. In fact, for most cases there the jet starts to spread a few D1 downstream of the exit plane. This is attributed to the recirculation zone created by the thick post of the inner jet. This recirculation zone has been seen experimentally and in the computations performed by Liu et. al.[9] who modeled two test conditions performed in our

lab. The spreading angle reported here is measured from the point where the jet starts to grow (~2 to 4 D1 downstream of the exit plane) to 10D1. Therefore this can be interpreted as an initial spread angle. Figure 3 shows a typical image and how the spreading angle is measured. Only $\alpha 1$ and $\alpha 4$ are visible and measured. The angles $\alpha 2$ and $\alpha 3$ although part of the shear layer are not visible in the backlit images. They are indicated to complete a conceptual picture required to compare the measurements with theoretical predictions as will be shown later.

Table 1. Summary of range of conditions for each pressure range .

Mean Chamber pressure, P (MPa)	Outer to inner jet Velocity ratio, VR	Outer to inner jet momentum flux ratio, MR	Mean inner jet mass flow rate (mg/s)	Mean Chamber temperature (K)	Mean Inner jet temperature (K)	Mean Outer jet temperature (K)
1.49	3.3 – 27	0.4 – 30	281	235	109	199
3.55	1.4 – 5.9	0.5 – 9.0	289	213	125	145
4.93	0.92 – 4.7	0.6 – 10.	293	229	137	173

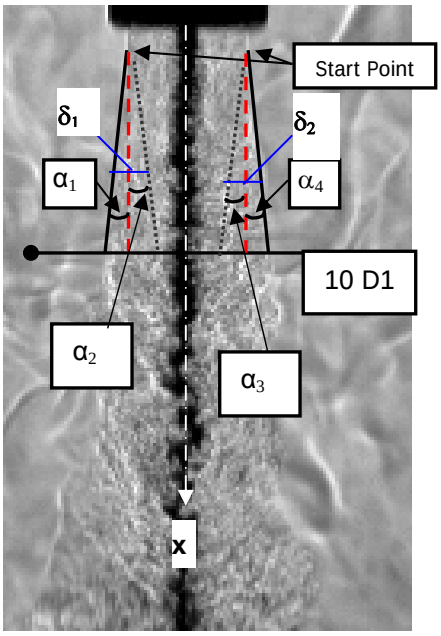

Figure 3. Typical image (from condition sub 7 in the Appendix) showing how the spreading angle is measured

There is very little previous work that we found directly in the area of spreading angles for shear coaxial jets, especially for cases where the exit pressures are much higher than atmospheric like in our case. Therefore, we first looked at the coaxial jet in a simplified form, which is consistent with the few data available for coaxial jets. We treat the outer jet/chamber shear layer as independent of the inner/outer jet shear layer. We then compare the outer jet/chamber shear layer with equation proposed for 2D shear layers and with axisymmetric single jets.

Furthermore, since the outer jet exits into a quiescent atmosphere, we first compare the data to single jets exiting into a quiescent atmosphere. Let's first take a look at how we measure the angles and relate them to theories for the visual growth of the shear layer $\frac{d\delta_v}{dx}$. If we look at Fig. 3 again, we see that for each of the two edges of the shear

layer seen in the backlit images (subscripts 1 and 2), we have for the visual growth of the shear layer δ_v (the v subscript is omitted for simplicity):

$$\frac{d\delta_1}{dx} = \delta_1' = \tan(\alpha_1) + \tan(\alpha_2) \quad \text{and} \tag{1}$$

$$\frac{d\delta_2}{dx} = \delta_2' = \tan(\alpha_3) + \tan(\alpha_4) \tag{2}$$

If all the angles are the same, then $\delta_1' = \delta_2' = 2\tan(\alpha_1)$. However, from the experiments we know this is not the case. The approximations we make by not measuring the four angles are as follows. First we can assume that $\alpha_1 \approx \alpha_2$ and $\alpha_3 \approx \alpha_4$ then for small angles we have,

$$\frac{\overline{d\delta}}{dx} \approx \tan(\alpha_1) + \tan(\alpha_4) \tag{3}$$

Where $\frac{\overline{d\delta}}{dx}$ is the mean value of the two measured shear layer thickness derivatives. On the other hand, a lot of literature reports the tangent of the total included angle ($\alpha_1 + \alpha_4$). We start again with equations (1) and (2) and assume all the angles to be small enough such that the approximation $\tan(\alpha) \approx \alpha$ applies. We also assume that $\alpha_2 = R_{12}\alpha_1$ and $\alpha_3 = R_{34}\alpha_4$. Then, accounting for possible asymmetries of the shear layers (for example Abromovich[10] found R~0.6 for plane jets exiting into a quiescent atmosphere) we have,

$$2\frac{\overline{d\delta}}{dx} \approx (1 + R_{12})\alpha_1 + (1 + R_{34})\alpha_4 \tag{4}$$

Since we have not found a theory to describe how R_{12} and R_{34} might differ from each other, for simplicity we assume them to be the same and equal to R since both shear layers have the same mean conditions. We then take the tangent of both sides and we obtain,

$$\tan(\alpha_1 + \alpha_4) \approx \tan(\frac{2}{1+R}\frac{\overline{d\delta}}{dx}) \approx \tan(c\frac{\overline{d\delta}}{dx}) \tag{5}$$

Here the only source of uncertainty is the value of R. For $0.6 < R < 1$, $1 < c < 1.25$. For simplicity, if we assume that $R = 1$ then

$$\tan(\alpha_1 + \alpha_4) \approx \tan(\frac{\overline{d\delta}}{dx}) \tag{6}$$

This equation is equivalent to equation (3) for small angles.

Now let's look at Fig. 4 which is a compilation of experimental data done by Chehroudi et. al.[5] on single jets with the current data and other data available for coaxial jets added. In this case the tangent of the total jet divergence angle is plotted against the chamber to injectant (single jets) or chamber to outer jet (coaxial jets) density

ratio. The data taken by Chehroudi for single jets in the same AFRL facility is marked by (*) in the legend. The coaxial jet data is labeled as Subcritical, Transcritical and Supercritical P. The first thing to notice is that there is little overlap on the ranges of (ρ_{ch} /ρ_{OJ}) for the coaxial and single jets. Also, the current data is consistently lower than the rest of data. We will look to that in more detail. It is useful to look in detail to some of the theoretical expressions presented in this figure. The first one is the prediction for the jet spreading angle made by Papamoschou and Roshko[3] for incompressible variable-density mixing layers. Even though this is for planar jets, Brown and Roshko[2] argue that the shear layer growth for a planar shear layer is approximately the same as for axisymmetric jets in the near field close to the injector exit plane. In their work[3,] they proposed,

$$\delta_v' = 0.17\left(\frac{\Delta U}{U_c}\right) = 0.17\left(\frac{U_1 - U_2}{U_c}\right) \tag{7}$$

where U_c is a convective velocity given by $U_c = (U_1\sqrt{\rho_1} + U_2\sqrt{\rho_2})/(\sqrt{\rho_1} + \sqrt{\rho_2})$ and the subscripts 1 and 2 refer to the two different mixing layers. That is, the visual shear layers are predicted to grow linearly with the delta U between the jets divided by a convective velocity which takes into account the density of the different jets. The constant 0.17 was obtained from the earlier work of Brown and Roshko[2]. The second equation used is not directly for the visual growth rate but rather for the vorticity growth, δ_w', derived by Dimotakis[4],

$$\delta_w' = \varepsilon\left(\frac{1-r}{1-s^{1/2}r}\right)\left[1 + s^{1/2} - \frac{1-s^{1/2}}{1+2.9(1+r)/(1-r)}\right] \tag{8}$$

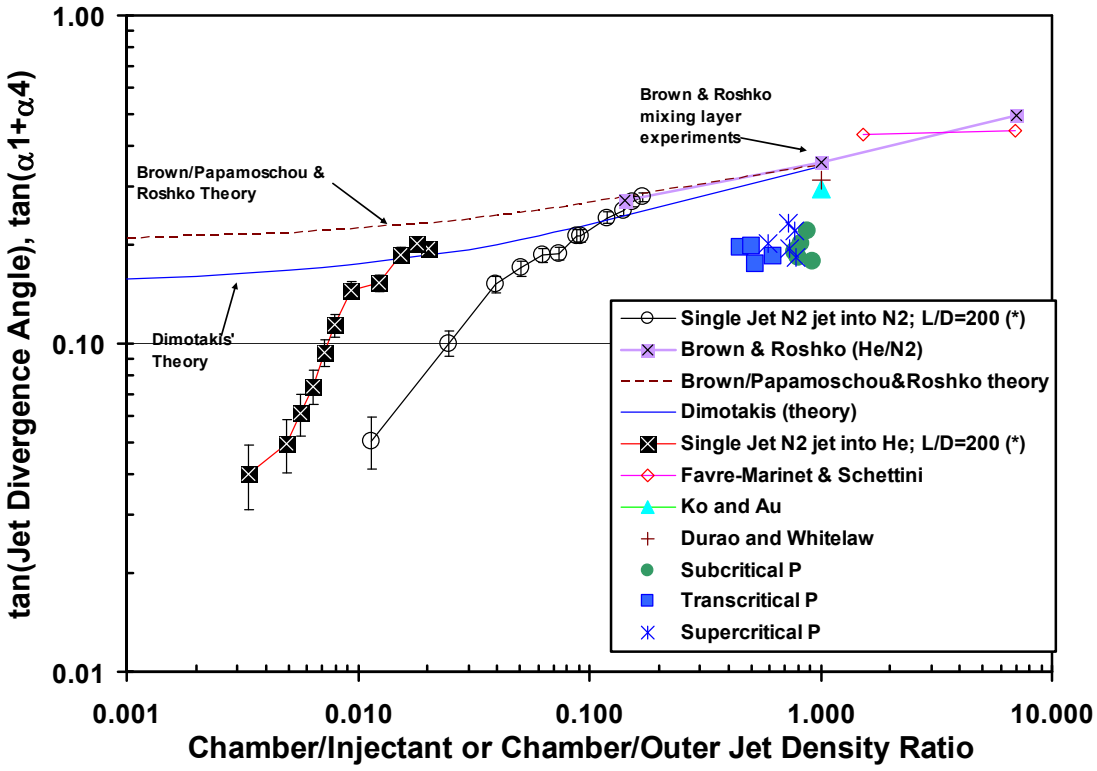

Figure 4. Spreading rate of the shear layer versus the chamber/injectant or chamber/outer jet density ratio for single and coaxial jets compared with different predictions for planar shear layers.

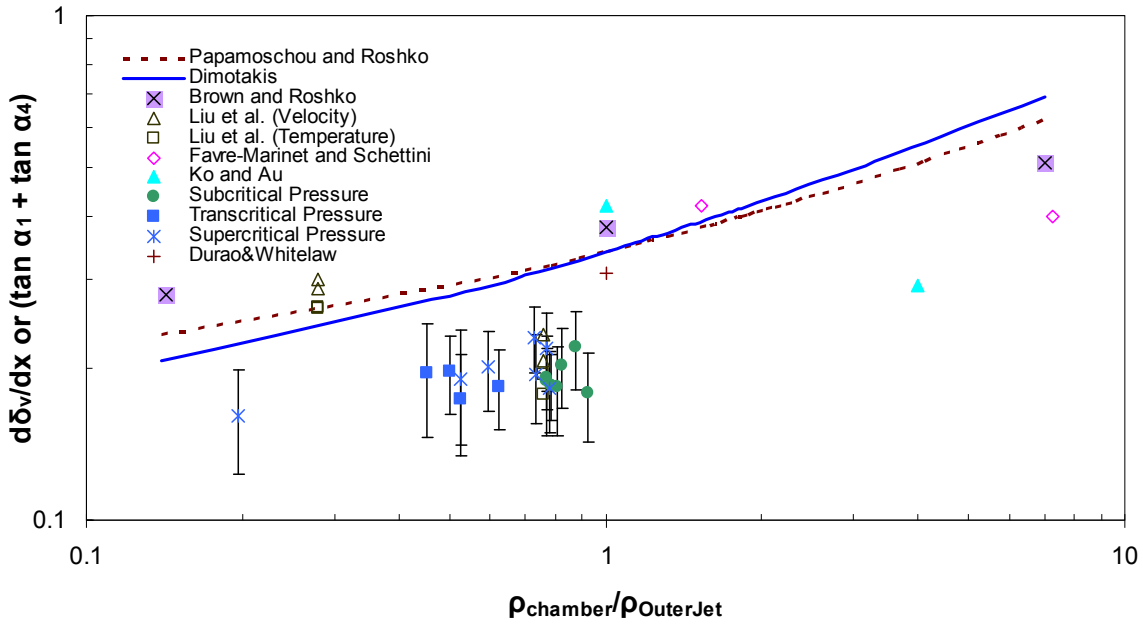

Figure 5. Spreading or growth rate of the shear layer versus the chamber-to-outer jet density ratio for coaxial jets compared with different predictions for planar shear layers with error bars.

where $r = U_2 / U_1$ and $s = \rho_2 / \rho_1$. It has been proposed [2,3] that $\delta'_v = 2\delta'_w$. For the case of round jets, Chehroudi et.al.[5] took $\varepsilon = 0.17/2$. Notice again that if U_2 / U_1 is zero δ'_w also becomes a function of ρ_2 / ρ_1 only. Brown and Roshko[2] also proposed for variable density planar mixing layers:

$$\delta'_v = A\left(\frac{U_1 - U_2}{U_1 + U_2}\right) \tag{9}$$

where A is 0.51, 0.38, and 0.28 for ρ_2 / ρ_1 being 7, 1, and 1/7 respectively. For the case of $U_2 = 0$ (quiescent condition), this reduces to three constants for the different ratios in density.

Now let's look at the present data. Fig.5 shows only coaxial data compared with the same theoretical predictions with error bars. Because the horizontal axis is the ratio of the chamber to the outer jet density, and since the chamber temperature and the outer temperature don't change very much within a given pressure range, then the data points run at sub, trans and supercritical pressures are reasonably well "separated". The data points from Liu et al.[9] are the results of their CFD analysis and were made from velocity and temperature mean profiles (color contours) found in their paper. The velocity contours included lines of constant velocity which made it easier to approximate the edge of the outer jet. The temperature profiles didn't have such lines so that measurements have larger uncertainty. However, these are presented here since they follow our experimental results closely and are the only data we were able to find so far on coaxial flows at supercritical conditions. The experimental data from Favre-Marinet et. al.[11] were made from density profiles in a variable density coaxial jet arrangement. The data from Ko & Au[12] and Durao & Whitelaw[13]are for gas-gas coaxial jets with density ratio of one and both are velocity based. Branam & Mayer[14] published a study where they compared different techniques to measure the shear layer growth angle for single round jets including supercritical conditions. They compared the results obtained from Raman and shadowgraph measurements with density profiles (50% ρ, 99% ρ) , temperature profiles (50% T, 99%T) as well as

computational velocity profiles (50% u, 99%u). They found that the differences between visual measurements and the 99%u, 99%T, and 99% ρ averaged to about 11%, 19% and 13% respectively. As different profiles are being used to estimate the spreading angle this provides a reference to assess the degree of agreement of the collected coaxial jet experimental and computational data with the one obtained here. The data presented here is fairly constant across the range of conditions studied with a mean growth rate value of 0.19 and a standard deviation of 0.02. The differences with other data (except Liu et al[9]) is more than 50% which is more than the differences expected due to the different measurement techniques use. One difference between these data and the others we compare against is that the thickness of the inner post is unusually large which affects the initial growth of the outer jet due to the large recirculation zone created downstream of the inner jet exit plane (recessed from the outer jet in this case). Also, while the data from other researchers is from gas-gas jets issuing into a gas, our data is liquid/gas at subcritical pressures issuing into a stagnant gas and one-phase at supercritical pressures issuing into a supercritical stagnant fluid. We will run gas-gas-gas conditions next in our lab and will show the results in a later paper.

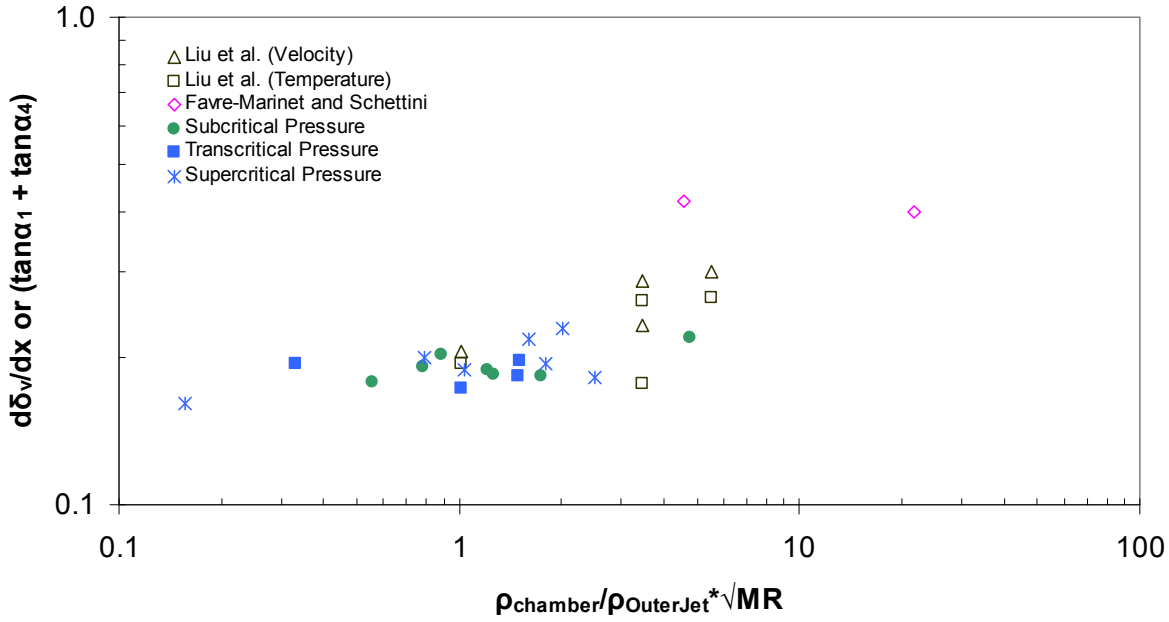

Figure 6. Spreading or growth rate of the shear layer versus the chamber-to-outer jet density ratio* MR for coaxial jets compared with other experimental and CFD data.

Finally, we present the same data in a different light considering the effects of the momentum flux ratio between the inner and outer jets. Figure 6 shows the spreading angle, or $\tan(\alpha_1)+\tan(\alpha_4)$ versus a parameter that includes effects from the outer and inner jet and the chamber, namely the ratio ρ_{ch}/ρ_{OJ} which is the main parameter controlling the shear layer growth into quiescent environment multiplied by the square root (sq. rt.) of MR. MR was chosen because it has been shown before [6,7,15] to be an important parameter controlling the mixing between the two jets. Also, it has been shown [6,7,15] that the length of the potential dark core grows approximately as the sq. rt. of the MR. Finally, the sq. rt. preserves the effects of the outer jet density in the proposed variable, which we believe is important for these cases. What stands out in this plot is that no longer are the different chamber P regimes in different regions of the x-axis. In fact, we have conditions at different chamber pressures that have the same value of $\rho_{ch}/\rho_{OJ} * \sqrt{MR}$ and give the same value for $\left[\tan(\alpha_1)+\tan(\alpha_4)\right]$. Since all the values for $\left[\tan(\alpha_1)+\tan(\alpha_4)\right]$obtained here are more or less constant we didn't expect to uncover any trends with the new x-variable. However, the new variable has relocated the rest of the data from other researchers in such a way that an

upward trend of the shear layer growth with the variable $\rho_{ch} / \rho_{OJ} * \sqrt{MR}$ seems to be emerging. Needless to say that additional work would be needed to confirm such a trend.

B. Dark Core Length with Two Acoustic Sources On

The second part of this paper concerns preliminary results obtained by transversely exciting the coaxial jet with two identical acoustic wave generating sources whose relative phase can be changed arbitrarily. Referring back to Fig. 1B which shows the two acoustics sources on the chamber, when the two sources have a zero degree phase angle, then the movement of the cones themselves could be described as "towards each other" as presented in Figure 7. At the other extreme, when the two sources are at 180 deg out of phase, then the motion could be seen as "chasing" each other. For all the cases, only the phase of the right resonator is changed with respect to the left resonator. Also, the two acoustic sources are fed with constant voltages throughout the phase changes. As mentioned earlier, we selected to start with two cases in the subcritical pressure regime based on previous experiments[6,7] which have shown that the greatest effect of acoustics, for the range of conditions studied in our lab, is for subcritical pressures. Within this regime the greatest percentage of reduction of the dark core length when the acoustics were turned on was for 1<MR<4. Therefore, we started with MR~1 and MR~2.6. Sample images from the case Sub8 (MR~2.6) at the different phase angles is presented in Fig. 8. The "no-acoustics" case is the baseline case with both sources off. When the two sources are on and in phase, the injector is located at a pressure antinode (since it is in the middle between the two sources) and the injector sees the least acoustic velocity perturbations. As the figure shows, the acoustic effects start to be visible in terms of the added bending to the inner jet and the growth of spreading angle. Notice that both the inner and outer jet bend with the acoustic field. The bending of the inner jet and outer jets continues to amplify, along with the spreading angle and shortening of the dark core, from 45 deg through 135 deg, reaching the most dramatic results at 135-180 deg. At 180 deg phase difference the dark core length is smallest. The trends reverse as we continue to change the phase angle from 180 deg to 360 deg (0 deg).

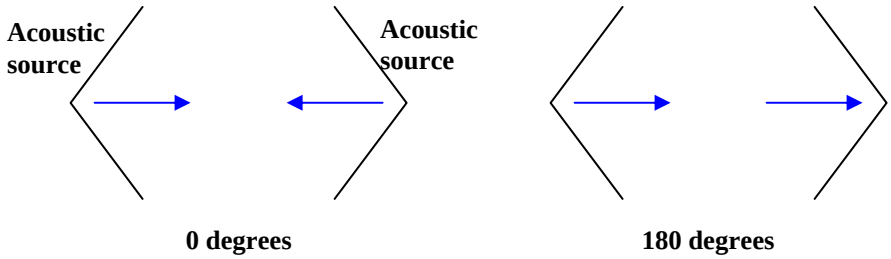

Figure 7. Schematic of the two acoustic sources at with phase angles of 0 and 180 deg between them.

The dark core lengths for cases sub7 (MR=1.0) and sub8 (MR=2.6) are shown in Figs. 9 and 10. The definitions used and techniques employed to measure the axial and curved dark core length are explained in detail in Leyva et. al.[7] The dark core lengths are measured from at least 1000 images automatically using a matlab subroutine based on the Otsu[16] technique to find a grayscale threshold which separates the inner core from the rest of the image. The axial length is the projection of the core onto the axial axis and the curved length is the total length of the core which takes into account the curvature produced by the acoustic excitation.

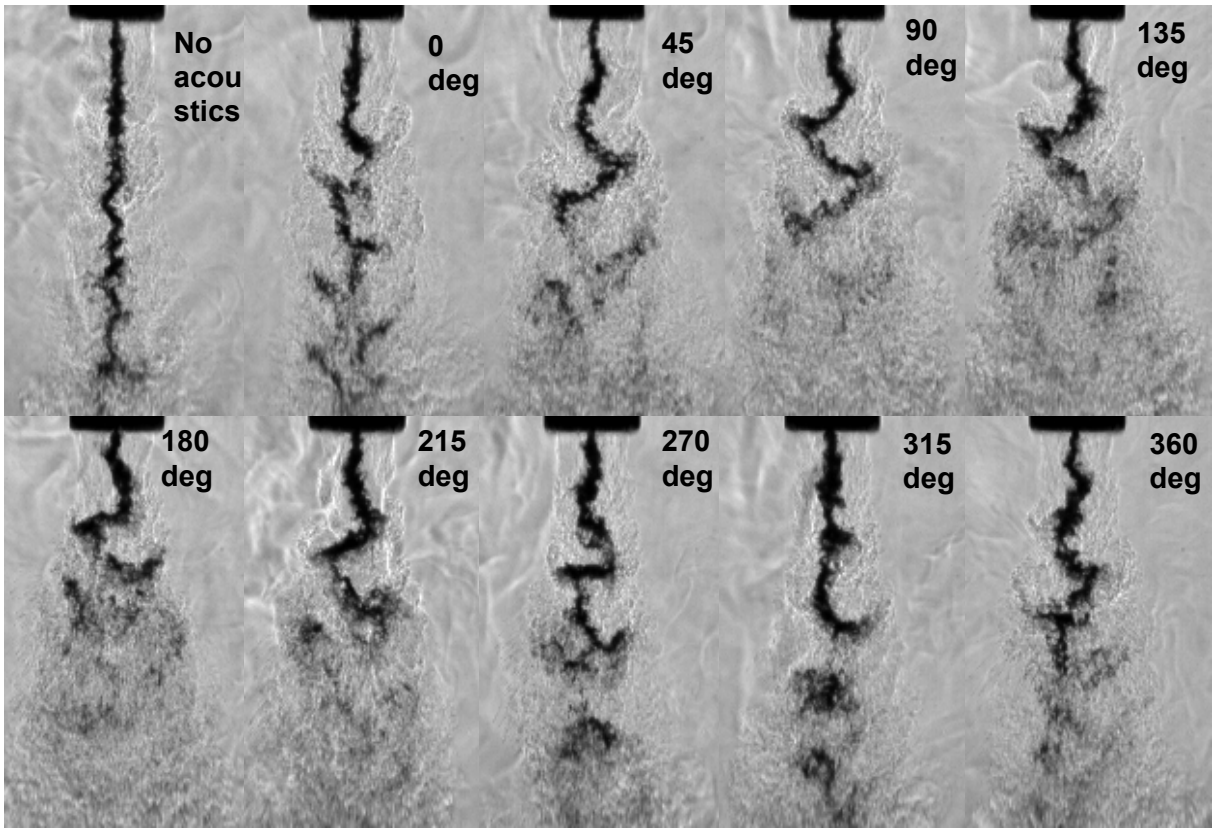

Figure 8. Sample images from Case Sub 8 with different phase angles between the two acoustic sources

As can be noted from Figs. 9 & 10, while there seems to be a periodic variation on the dark core as the phase angle between the two signals changes from 0-360 deg, most of the data falls within the error bars (± 1 standard deviation) and therefore we can't definitely say that such a trend exists. As we would expect the dark core length is longest when there are no acoustic disturbances as also seen in Fig. 8. Next, when one acoustic source is turned on the dark core length decreases as observed in previous studies. For the case of Fig. 10 for the plot of AxialL/D there is a statistical difference between the baseline case with no acoustics and the case with 180 deg phase difference, which also corresponds to the lowest acoustic $\Delta p/p$ measured (~0.7%). Here Δp is the RMS value of the pressure fluctuations.

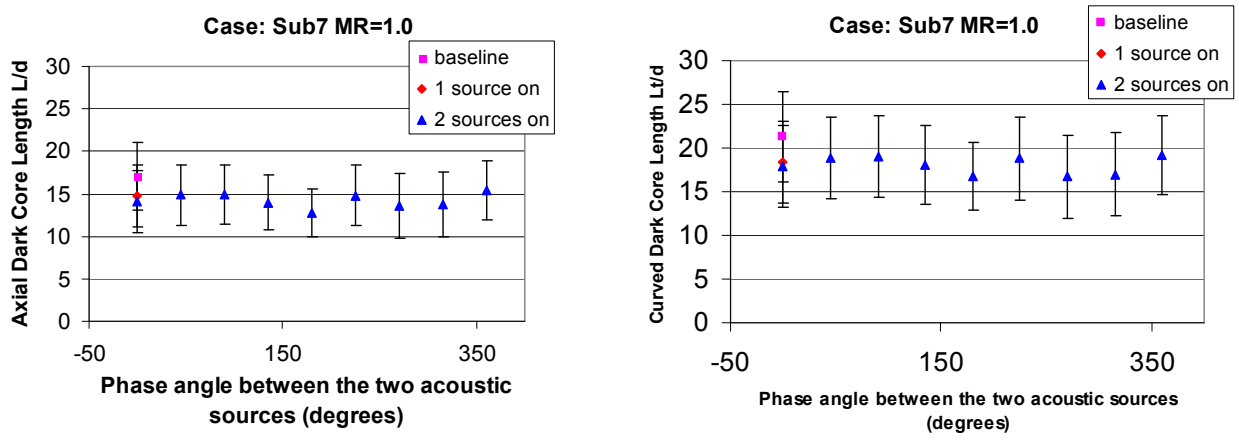

Figure 9. Variation of the axial and curved dark core length for subcritical pressure and MR=1.0 as a function of the phase angle between two acoustic resonators.

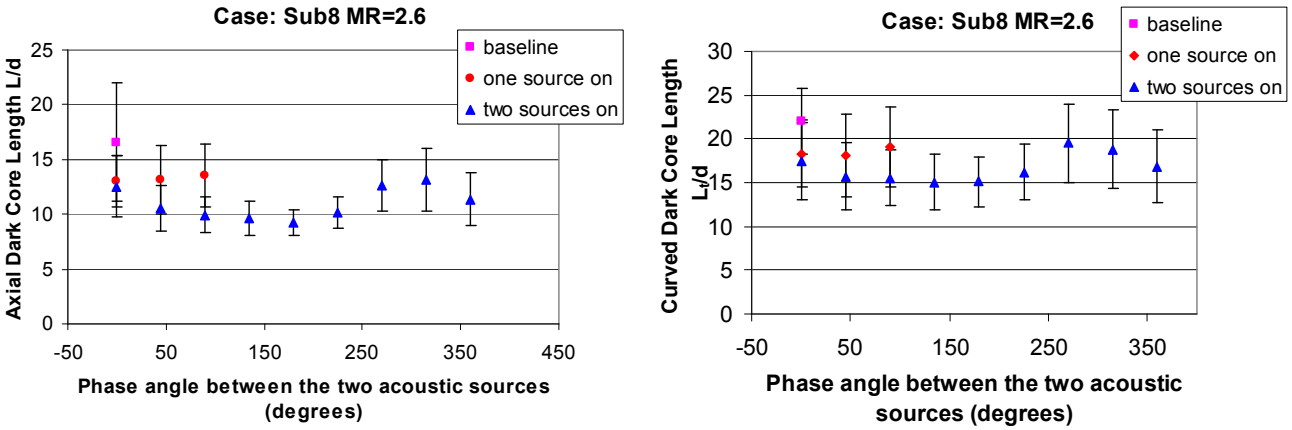

Figure 10. Variation of the axial and curved dark core length for subcritical pressure and MR=2.6 as a function of the phase angle between two acoustic resonators

For the same case the maximum dark core occurs at around 315 deg, corresponding to $\Delta p/p$ ~1.2%. These changes in $\Delta p/p$ are entirely due to the phase angle since the driving voltage for the two sources is constant throughout the phase sweep. Since the dark core is the longest here, one can say that the acoustics had little impact on the mixing of the two layers. We expect this to be close to a pressure antinodes and therefore to have the weakest acoustic velocity field. This implies, as one would expect that the maximum effect of the acoustic field on the jet mixing is through the velocity field and not the pressure field. This is furthered corroborated by the fact that in the set up with one acoustic resonator the jet was positioned near the pressure node for the same frequency used with two sources. For that case when the acoustics were turned on, we obtained about the same difference in the core

length as the difference observed here between the baseline case and the case at 180 deg. A more thorough study is underway where the pressure will be changed to trans and supercritical values and more MR values will be run.

IV. Conclusions

Extensive experimental data was presented on the growth rate or spreading angle of the outer jet of a coaxial jet flow exiting into a quiescent atmosphere. N_2 was used for both the inner and outer jets and the chamber environment. The chamber pressure varied from 1.5 to 5.0 MPa. When the chamber pressure is subcritical the flow is two-phase (liquid core and gaseous outer jet) and when the pressure is supercritical both jets are in the supercritical regime and we have one-phase flow. It was found that the near-field outer jet spreading angle for all cases was fairly constant (mean=0.19 with standard deviation of 0.02). This value was compared with theoretical predictions obtained for 2D shear layers of variable density flows for gaseous flows and with other experimental data for single jets and coaxial gas-gas jets issuing into a gas. The growth rate or spreading angle for the present data is consistently lower than the theoretical predictions and the other experimental data for coaxial jets. An important difference might be the thickness of the inner jet tube, which produces a big recirculation zone directly downstream of the inner jet exit plane and might have a significant effect on the outer jet spreading angle. The second part of the paper presented preliminary data on the effects of varying the phase angle between two acoustics sources that transversely excite the coaxial jet at subcritical pressures. In effect, what is varying is the magnitude and phase of the velocity and pressure field at the location of the jet. The acoustic frequency is about 3 kHz. The level of the acoustic $\Delta p/p$ was between 0.7 to 1.3 % depending on the phase between the two acoustic sources. It was found that the dark core length is shortest for the lowest amplitudes of $\Delta p/p$. This implies that the maximum enhancement on mixing, and hence decrease on the dark core, corresponds to maximum acoustic velocity fluctuations. An experimental investigation is also underway to thoroughly study these effects.

Appendix

Table A1. Properties of the coaxial jets of the cases presented in this study

	$T_{chamber}$ (K)	$\rho_{chamber}$ (kg/m^3)	$P_{chamber}$ (MPa)	T_{outer} (K)	$\dot{m}_{outer}$ (mg/s)	ρ_{outer} (kg/m^3)	u_{outer} (m/s)	T_{inner} (K)	$\dot{m}_{inner}$ (mg/s)	ρ_{inner} (kg/m^3)	u_{inner} (m/s)	VR	MR	tan α1 + tan α4
sub1	252	19.9	1.48	235	395	21.5	7.03	108	280	638	2.17	3.27	0.360	0.18
sub2	242	21.1	1.50	202	787	25.7	11.7	110	280	622	2.22	5.31	1.16	0.20
sub3	242	21.3	1.50	198	1590	26.4	23.1	110	281	622	2.23	10.5	4.64	0.18
sub4	240	21.2	1.49	213	2950	24.2	46.7	110	281	622	2.23	21.1	17.4	0.21
sub5	232	22.1	1.50	206	3940	25.2	59.8	110	280	622	2.22	27.1	29.8	0.22
sub6	213	24.2	1.49	170	1250	31.4	15.3	109	280	630	2.19	7.02	2.45	0.19
sub7	231	22.2	1.50	183	789	28.8	10.5	109	283	630	2.21	4.77	1.04	0.19
sub8	226	21.9	1.45	183	1230	27.8	16.9	109	284	629	2.23	7.63	2.57	0.19
trans1	216	58.7	3.57	138	1410	130	4.14	125	291	482	2.98	1.40	0.530	0.20
trans2	210	60.3	3.54	143	3450	115	11.5	123	292	508	2.84	4.09	3.77	0.17
trans3	215	58.7	3.54	157	4040	94.3	16.4	126	286	442	3.19	5.17	5.72	0.18
trans4	209	60.5	3.54	141	5650	121	17.8	125	287	465	3.05	5.89	9.06	0.20
sup1	245	70.2	4.92	172	2810	118	9.10	133	293	373	3.88	2.36	1.77	0.20
sup2	236	73.8	4.94	195	5750	95.7	23.0	147	295	179	8.12	2.86	4.35	0.22
sup3	225	78.7	4.95	183	5810	107	20.9	138	292	264	5.45	3.86	6.00	0.19
sup4	236	72.9	4.89	188	7050	100	26.9	141	293	214	6.76	4.01	7.55	0.23
sup5	227	77.1	4.93	191	8140	99.0	31.5	141	293	216	6.69	4.74	10.3	0.18
sup6	224	78.8	4.93	132	2580	402	2.45	125	293	535	2.71	0.914	0.628	0.16
sup7	209	86.7	4.96	150	4620	165	10.7	132	294	423	3.42	3.15	3.87	0.19

Acknowledgments

The authors would like to recognize Randy Harvey for his invaluable contributions on running and maintaining the facility. This work is sponsored by AFOSR under Mitat Birkan, program manager.

References

1. Oschwald, M., Smith, J. J., Branam, R., Hussong, J., Schik, A., Chehroudi, B., Talley, D., "Injection of Fluids into Supercritical Environments", *Combustion Science and Technology*, Vol. 178, No. 1-3, 2006, pp. 49-100.
2. Brown, G., Roshko, A., "On density effects and large structure in turbulent mixing layers"; J. Fluid Mech, Vol. 64 part 4, 1974, pp. 775-816
3. Papamoschou D., Roshko, A., ''The compressible turbulent shear layer:an experimental study,'' J. Fluid Mech. Vol. 197, No. 453 1988
4. Dimotakis, P. E., "Two-Dimensional Shear Layer Entrainment", AIAA Journal, Vol 24, No. 11, Nov. 1986, pp. 1791-1796
5. Chehroudi, B., Talley, D., Coy, E., "Visual characteristics and initial growth rates of round cryogenic jets at subcritical and supercritical pressure", Physics of Fluids, Vol. 14, No. 2, February 2002, pp. 851-861.
6. Leyva, I. A., Chehroudi, B., Talley, D., "Dark-core analysis of Coaxial Injectors at Sub-, Near-, and Supercritical Conditions in a Transverse Acoustic Field", *54th JANNAF Meeting*, Denver, CO, May 14-18, 2007.
7. Leyva, I. A., Chehroudi, B., Talley, D., "Dark-core analysis of Coaxial Injectors at Sub-, Near-, and Supercritical Conditions in a Transverse Acoustic Field", *AIAA-2007-5456*
8. REFPROP, Reference Fluid Thermodynamic and Transport Properties, Software Package, Ver. 7.0, NIST, U.S. Department of Commerce, Gaithersburg, MD, 2002.

9. Liu T., Zong, N., Yang, V., "Dynamics of Shear-Coaxial Cryogenic Nitrogen Jets with Acoustic Excitation under Supercritical Conditions", AIAA 2006-759.
10. Abramovich, G. N., *The Theory of Turbulent Jets*, MIT Press, Cambridge,1963.
11. Favre-Marinet, M., Camano Schettini, E.B., "The density field of coaxial jets with large velocity ratio and large density differences", Int. J. of Heat and Mass Transfer, 44 (2001) pp. 1913-1924
12. Ko, N. W. M. , Au, H., "*Initial region of subsonic coaxial jets*", J of Fluids Engineering, June 1981, vol. 103, pp 335-338.
13. Durao, D. and Whitelaw, J. H. Turbulent mixing in the developing region of coaxial jets", J of Fluids Engineering, Sept, 1973, pp.467-473.
14. Branam, R., Mayer, W., "Characterization of Cryogenic Injection at Supercitical Pressure", JPP Vol. 19, No. 3, May-June 2003 pp. 342-354
15. Davis, D. W., Chehroudi, B., "Measurements in an acoustically driven coaxial jet under sub-, near-, and supercritical conditions", *JPP*, Vol. 23, No. 2, March- April 2007
16. Otsu, N., "A threshold selection method from gray-level histograms", *IEEE transactions on Systems, Man, and Cybernetics*, Vol. 9, No. 1, 1979, pp. 62-66.